ARC Journal of Radiology and Medical Imaging
Volume 4, Issue 2, PP 19-25
www.arcjournals.org

Volumes of Midbrain Nuclei in Pantothenate-Kinase Associated Neurodegeneration (PKAN) Dystonia

Peter Stoeter[1*], Pedro Roa[2], Bernd Foerster[1], Ysberlin Reynoso-Rivas[1], Jorge Romero-Reynoso[1], Herwin Speckter[1], Cesar F. Gonzalez[1]

[1]*Department of Radiology, CEDIMAT, Plaza de la Salud, Santo Domingo, Dominican Repulic*

[2]*Department of Neurology, CEDIMAT, Santo Domingo, Dominican Republic*

Corresponding Author:** ***Peter Stoeter*, Department of Radiology, CEDIMAT, Plaza de la Salud, Santo Domingo, Dominican Repulic* ***Email:*** *peter.stoeter@gmx.de*

Abstract

Background: *In Pantothenate-Kinase Associated Neurodegeneration (PKAN) dystonia, midbrain nuclei have been reported to participate in accumulation of iron in a similar way as globus pallidus, where it is known as the "eye-of-the-tiger" sign. Volume changes of midbrain nuclei have not been reported by now, but might well contribute to pathophysiology of this hyperkinetic movement disorder.*

Material and Method: *In 14 patients affected by PKAN and in 13 age-matched controls, nucleus ruber, substantia nigra and nucleus subthalamicus were segmented from T1- and T2-weighted Magnetic Resonance Images. In addition, Quantitative Susceptibility Mapping of these nuclei was performed to look if a possibly increased accumulation of iron of these nuclei could influence the volumetric results.*

Results: *Substantia nigra was smaller in patients as compared to controls with a significant volume reduction of 17.8% ($p<0.01$) on the left and of 11.2% on the right side. QSM values were similar in patients and controls, without correlation to volumetric results.*

Conclusion: *Because influence of iron accumulation in midbrain nuclei could be excluded in this study, volumetric results are reliable. However, a correlation between volume loss of substantia nigra and clinical data could not be demonstrated. Further volumetric studies in PKAN including the cerebellum and more clinical data are needed to clarify the role of motor centers outside the basal ganglia in PKAN.*

Keywords: *Pantothenate-Kinase Associated Neurodegeneration, Volumetry, Midbrain Nuclei*

1. Introduction

Pantothenate-Kinase Associated Neurodegeneration (PKAN) is an inherited, autosomal-recessive condition, which is characterized clinically by progressive distonía [1]. It belongs to the group of orphan diseases with a prevalence of 1:1-3,000,000 cases. The primary genetic defect has been localized to the PANK2 gene and induces impairment in the production of Acetyl-Coenzyme A resulting in formation of deficient mitochondrial acyl carrier protein and finally in dyshomeostasis and accumulation of iron [2]. In Magnetic Resonance Imaging (MRI), patients present the typical "eye-of-the-tiger" sign, which consists of a bright lesion in the anterior part of the globus pallidus surrounded by an area of signal loss due to excessive accumulation of iron [3,4].

MRI studies of PKAN patients have concentrated mainly on measurement of changes of T2star time resp. susceptibility of the basal ganglia [5-7]. Structural MRI examinations comparing grey and white matter volumes between PKAN patients to controls are not as frequent and have reported deviations of the volume of basal ganglia in children and of some cortical areas in adults [8] as well as reduction of frontal white matter integrity [9]. To best of our knowledge, volumetric measurements of midbrain nuclei never have been reported so far, although these nuclei play an important part in the pathophysiology of other movement disorders like Parkinson's disease, and the appearance of Parkinsonian symptoms during later stages of PKAN is well-known [10].

The present study was undertaken to look for volumetric differences of the midbrain nuclei which possibly may contribute to the pathophysiologic understanding of the dystonic movement disorder in a group of PKAN patients from the Dominican Republic using a recently published program of segmentation of subcortical structures [11]. At the same time, we measured the susceptibility of these nuclei, which might be increased in PKAN similar as in globus pallidus [12], in order to look if this

parameter might eventually influence our volumetric results.

2. Material and Methods

This prospective study had been approved by the local Ethics Committee, and informed consent had been received from all participants resp. their parents.

2.1. Patients and Controls

Apart from genetic confirmation of PKAN, a main criterion for inclusion of patients was absence of movement artifact in the highly susceptible T2star-weighted and other images. Thus, 14 patients, 9 females and 5 males, of a mean age of 24.4 (10.3 to 50.4) years and 13 healthy age-matched controls, 10 females and 3 males not related to hospital staff, of a mean age of 21.9 (11.4 to 55.6) years were included. Mean age of onset of symptoms was 10.6 ± 3.6 years and mean duration of symptoms 13.6 ± 11.2 years. On neurological examination, patients presented different types of dystonia, with involvement of extremities, trunk and/or the oro-pharyngeal region, showing a mean score on the Burke-Fahn-Marsden (BFM) dystonia scale of 34.5 ± 21.4 points and of 12.3 ± 6.7 points on the BMF disability scale (table 1).

Table1. *Patients, Controls, and clinical data*

	N	Age at Examination	Age at Onset of PKAN	Duration of Symptoms	Dystonia (BFM scale)	Disability (BFM scale)
Patients	14	24.2 (10.3 - 50.4)	10.6 ± 3.6	13.6 ± 11.2	34.5 ± 21.4	12.3 ± 6.7
Controls	13	21.9 (11.4 – 55.6)				

2.2. MR Imaging

All scans were measured on the same Philips 3T Achieva scanner, release 3.2, 8-channel head coil, and included the sequences mentioned below. Scans showing obvious movement artifacts were excluded from further evaluation.

- T1-weighted MPRAGE: 3-dimensional Turbo Field Echo, TR/TE=6.73/3.11 ms, 180 sagittal slices, voxel size 1mm^3.
- T2-weighted Spin-Echo (SE): TR/TE 3022/80 ms, 70 axial slices, slice thickness 2mm, pixel size 0.34x0.34 mm.
- Quantitative Susceptibility Mapping (QSM): T1 weighted 3D FFE sequence, 50 transversal slices of 1.3 mm thickness centered to the basal ganglia. TR 50 ms, TE 4.6 ms, flip angle 12°. 10 echoes with 4.6 ms spacing. Pixel size 1.3x1.3 mm. For calculation of QSM maps, we applied the MEDI (Morphology-Enabled Dipole Inversion) toolbox (http://weill.cornell. edu/ mri/QSM/MEDI_ toolbox) running on MATLAB.

2.3. Evaluation of Data

From T1- and T2-weighted data, red nucleus, substantia nigra and suthalamic nucleus were segmented using the Multimodal Image Segmentation Tool (MIST), developed by Visser et al. [11]. The program runs under Functional MRIB Library (FSL, http://fsl.fmrib.ox.ac.uk/). This method is able to use multiple image modalities simultaneously and a single reference segmentation for initialisation, without the need for a manually labelled training set. It models intensity profiles in multiple images around the boundaries of the structure after nonlinear registration. It is trained using a set of unlabelled training data, which are the same images used for segmentation, and it can automatically infer the location of the physical boundary using user-specified priors.

Volumes of masks of segmented red nuclei, subthalamic nuclei and substanciae nigrae were measured using the VOI facility of the MRIcron platform (www.nitrc.org/projects/mricron), all normalized to an intracranial volume of 1400 cm^3. The same masks were used to measure QSM values from co-registrated QSM maps. Normalized volumes were compared between patients and controls by 2-paired t-test. In patients, volumes were corrected for age and correlated to clinical data as (i) age at onset and (ii) duration of dystonic symptoms and values on the (iii) dystonia and (iv) disability scales using partial correlation analysis of the statistical package SPSS 15.0 (SPSS, Inc., Chicago, IL, USA).

In order to look for a possible influence of susceptibility values of mesencephalic nuclei on the volumetric results, we calculated a partial correlation analysis of volumes of nuclei to QSM values from all included subjects, corrected for status of subject belonging to the patient or the control group.

Significance was accepted on a 95% level, corrected for False Detection Rate (FDR, www. Sdm project.com/utilities/?show=FDR).

3. Results

Comparison of midbrain nuclei of patients and controls showed important volume reductions of the substantia nigra of 0.082cm^3 or 17.8% on the left and of 0.055 cm^3 or 11.2% on the right,

reaching significance (p<0.01, FDR corrected) on the left and showing a tendency to significance (P=0.082, FDR corrected) on the right (table 2, Fig. 1). The two other nuclei showed similar volumes in patients and controls (red nucleus around 0.3 cm^3 and subthalamic nucleus around 0.06 cm^3).

Table2. *Volumes and QSM values of patients and controls*

		Nucl. ruber L	Subst. nigra L	Nucl. subth. L	Nucl. ruber R	Subst. nigra R	Nucl. suthal. R
Patients	Volumes (cm^3)	0.291 ± 0.047	0.378 ± 0.062 *	0.054 ± 0.017	0.316 ± 0.052	0.434 ± 0.077	0.076 ± 0.022
	QSM values	18.79 ± 55.99	9.6 ± 38.34	32.18 ± 67	31.18 ± 36.19	-10 ± 36.45	62.41 ± 47.52 **
Controls	Volume (cm^3)	0.291 ± 0.036	0.460 ± 0.041 *	0.050 ± 0.009	0.322 ± 0.038	0.489 ± 0.050	0.072 ± 0.008
	QSM values	14.61 ± 27.64	35.26 ± 49.85	-11.95 19.14±	23.93 ± 36.25	25.45 ± 46.46	-40.5 ± 46.31 **

The left substantia nigra is significantly smaller in patients (, p < 0.01, FDR corr.). The QSM values of the right nucleus subthalamicus are significantly higher in patients (**, p < 0.001, FDR corr.).*

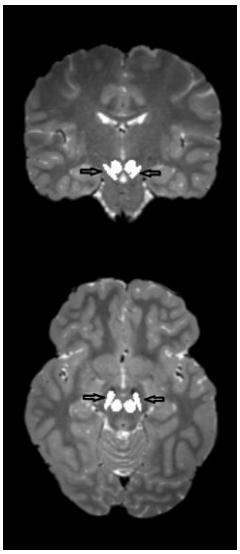

1(a)

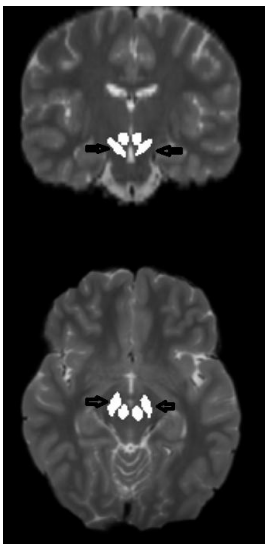

1(b)

Fig1. *Masks of red nuclei and substantiae nigrae in patient and control. Masks of red nuclei and substantiae nigrae (arrows) were overlaid on T2-weighted images in coronal (upper images) and transversal projection (lower images). Female patient, 11.4 years old (a), and female control, 13.5 years old (b)*

There were no significant correlations between volumes of midbrain nuclei and clinical parameters as age at onset and duration of symptoms and scaling on the BMF dystonia and disability scale. The highest Correlation Coefficients (CC) showed the relation between the left and right substantia nigra and the dystonia scaling values (0.450 on the left and 0.474 on the right), but without reaching significance (p=0.123 and p=116, uncorrected).

QSM values of midbrain nuclei were quite similar between patients and controls with the exception of the right subthalamic nuclei, where patients reached the highest values of all (62.41 units) as compared to -40.5 units in controls. This difference was significant (p<0.001, FDR corrected).

CCs between volumes of midbrain nuclei and their QSM values in patients and controls were calculated to look for internal dependence of both parameters and were negative in all three nuclei: CC= -0.220 for the red nuclei, CC= -0.050 for the substantiae nigrae and CC= -0.028 for the subthalamic nuclei. All CCs stayed well below the level of significance.

4. Discussion

To best of our knowledge, this is the first study to compare the volumes of midbrain nuclei between PKAN patients and healthy controls using a segmentation program based on T1- as well as on T2-weighted images. Segmentation techniques using just T1-weighted images perform well in some subcortical structures with high contrast to surrounding white matter as the putamen and caudate nucleus, but are less reliable in other areas without well-contrasted borders like globus pallidus or red nucleus [13]. Including a second image modality as T2-weighted data compares favorably to these conventional methods and has shown to produce consistent results that correspond well with manual segmentations [14].

We deliberately did not include further images such as T2star-weighted sequences, into the analysis because due to their higher sensitivity to iron accumulations, results of automated and manual segmentation procedures based on these sequences have been shown to be less accurate [15]. Our initial concern that problems with susceptibility changes of areas like the “tiger’s eye” might influence volume measurements in T2-weighted images, was not justified, because we did not see any relevant correlations between measured volumes and their QSM values. In addition, susceptibility of midbrain nuclei was not significantly different in patients and controls with exception of the right subthalamic nucleus. Although iron accumulation has been reported in the substantia nigra in PKAN patients [16]), midbrain nuclei usually are less affected in this condition than in other forms of Neurodegeneration with Brain Iron Accumulation (NBIA) [17, 18].

Results showed a significant volume reduction of the left sustantia nigra in patients (17.8%) and a (non-significant) tendency to smaller volumes on the right side in PKAN patients, whereas volumes of red nuclei and of subthalamic nuclei were similar to control values. This finding has not been reported before, because examinations of midbrain nuclei in PKAN so far have concentrated on demonstration of increased content of iron [19-21].

Reliability of the segmentation method applied in this study is underlined by the fact that in controls, volumes of red nucleus, sustantia nigra and subthalamic nucleus fit well to the range of normal values as measured by another segmentation program of midbrain nuclei based on T2-weighted images alone (www.volbrain.upv.es [22]): there, red nucleus occupied around 0.022%, sustantia nigra around 0.034% and subthalamic nucleus around 0.004% of Total Intracranial Volume (TIV). Volume measurements of the substantia nigra, confined to the pars compacta, based on histology and 9.4 Tesla MRI analysis, showed volumes of this part of the nucleus of 211.3 cm^3 in controls [23]. This fits as well to our results, which include the whole nucleus. Volumetry of subthalamic nuclei gave varying results, depending on the method used, with larger volumes measured from histology than from MRI. Based on images from a 3T scanner and an average of masks of raters, the value of 0.099 cm^3 is in the range of our results [24].

Unfortunately, the segmentation program applied does not differentiate between pars compacta and pars reticularis, which is an important issue in other movement disorders as in Parkinson’s disease [23, 25]. Connections of sustantia nigra to the striatum and from there through direct or indirect (via the subthalamic nucleus) connections to the globus pallidus might be of less importance because in PKAN, this nucleus is affected by the primary lesion. However, a direct inhibitory GABAergic pathway from the sustantia nigra to the motor

nuclei of the thalamus might be involved [26-28]. Thus, a reduced activity of substantia nigra, which might go along with volume reduction, could well contribute to the hyperkinetic movements seen in PKAN dystonia.

Although the lack of a correlation between volume loss of midbrain nuclei and clinical parameters does not support the view of an important influence of these structures on expression of clinical symptoms, this lack of evidence might be due to the limited number of participants in this study. But considering the rarity of the condition and the necessity to exclude scans with motion artifacts, a larger group size could not be achieved. Mainly older patients affected by PKAN of the late onset type are known to develop Parkinsonian signs like freezing of movements and gait [10, 29]. However, these symptoms were not assessed quantitatively by special scaling in the clinical part of this study.

5. Conclusion

This volumetric study was able to demonstrate for the first time a volume reduction of substantia nigra in PKAN patients. However - possibly due to the limited number of participants- a correlation of clinical data could not be demonstrated. Further volumetric studies including more participants, further brain areas as the cerebellum and more clinical data are needed to clarify participation of motor centers outside the basal ganglia in this condition.

Acknowledgments

The authors like to thank CEDIMAT and the Foundation Dr. Juan Ml. Taveras for generously supporting our social PKAN project in the Dominican Republic.

Authors' Contribution

All authors have made substantial contributions acquisition analysis and interpretation of data, have been involved in drafting and revising the manuscript and have given final approval of the present version to be published.

Ethical Standard

All procedures involving human participants were performed in accordance with the ethical standards of the institutional and/or national research committee and with the 1975 Helsinki declaration and its later amendments or comparable ethical standards.

References

[1] Hayflick SJ, Westaway SK, Levinson B, Zhou B, Johnson MA, Ching KH, Gitschier J. Genetic, clinical, and radiographic delineation of Hallervorden-Spatz syndrome. N Engl J Med. 2003 Jan 2;348(1):33-40.

[2] Lambrechts RA, Schepers H, Yu Y, van der Zwaag M, Autio KJ, Vieira-Lara MA, Bakker BM, Tijssen MA, Hayflick SJ, Grzeschik NA, Sibon OC. CoA-dependent activation of mitochondrial acyl carrier protein links four neurodegenerative diseases. EMBO Mol Med. 2019 Dec;11(12):e10488. doi: 10.15252/ emmm.201910488.

[3] Hayflick SJ, Hartman M, Coryell J, Gitschier J, Rowley H. Brain MRI in Neurodegeneration with Brain Iron Accumulation with and without *PANK2* Mutations. AJNR Am J Neuroradiol. 2006; 27(6): 1230–1233.

[4] Delgado RF, Sanchez PR, Speckter H, Then EP, Jimenez R, Oviedo J, et al. Missense PANK2 mutation without "Eye of the tiger" sign: MR findings in a large group of patients with pantothenate kinase-associated neurodegeneration (PKAN). J Magn Reson Imaging 2012;35:788-94.

[5] Gregory A, Hayflick SJ. Neurodegeneration with brain iron accumulation. Folia Neuropathol. 2005;43(4):286-96.

[6] Vilchez-Abreu C, Roa-Sanchez P, Fermin-Delgado R, Speckter H, Perez-Then E, Oviedo J, Stoeter P. El signo del "Ojo del Tigre" en resonancia magnética: cambios relacionados con la edad. Anal Radiol Mexico 2013;3:189-196

[7] Marshall RD, Collins A, Escolar ML, Jinnah HA, Klopstock T, Kruer MC, Videnovic A, Robichaux-Viehoever A, Burns C, Swett LL, Revicki A, Bender RH, Lenderking WR. Diagnostic and clinical experience of patients with pantothenate kinase-associated neurodegeneration. Orphanet J Rare Dis. 2019; 14: 174. doi: 10.1186/s13023-019-1142-1

[8] Rodriguez-Raecke R, Roa-Sanchez P, Speckter H, Fermin-Delgado R, Perez-Then E, Oviedo J, Stoeter P. Grey matter alterations in patients with Pantothenate Kinase-Associated Neurodegeneration (PKAN). Parkinsonism Relat Disord. 2014 Sep;20(9):975-9. doi: 10.1016/j.parkreldis.2014.06.005.

[9] Stoeter P, Roa-Sanchez P, Speckter H, Perez-Then E, Foerster B, Vilchez C et al. Changes of cerebral white matter in patients suffering from Pantothenate Kinase-Associated Neurodegeneration (PKAN): A diffusion tensor imaging (DTI) study. Parkinsonism Relat Disord. 2015;21:577-581. doi: 10.1016/ j.park reldis.2015.03.009.

[10] Lee JH, Park J, Ryu HS, Park H, Kim YE, Hong JY, Nam SO, SungYH, Lee SH, Lee JY, Lee MJ, Kim TH, Lyoo CH, Chung SJ, Koh SB, Lee PH, Cho JW, Park MY, Kim YJ, Sohn YH, Jeon BS, MS Lee. Clinical Heterogeneity of Atypical Pantothenate Kinase-Associated Neurodegeneration in Koreans. J Mov Disord. 2016 Jan; 9(1): 20–27. Published online 2016 Jan 25. doi: 10.14802/jmd.15058

[11] Visser E, Keuken MC, Douaud G, Gaura V, Bachoud-Levi AC, Remy P, Forstmann BU, Jenkinson M. Automatic segmentation of the striatum and globus pallidus using MIST: Multimodal Image Segmentation Tool. Neuroimage. 2016 Jan 15;125:479-497. doi: 10. 1016/j.neuroimage.2015.10.013.

[12] Roa P, Bido , Foerster B, Speckter H, González CF, Oviedo J, Stoeter P. Evaluation of the "Tiger's Eye" by Quantitative Susceptibility Imaging. ARC Journal of Radiology and Medical Imaging. 2017; 2(2): 7-11.

[13] Ewert S, Horn A, Finkel F, Li N, Kühn AA, Herrington TM. Optimization and comparative evaluation of nonlinear deformation algorithms for atlas-based segmentation of DBS target nuclei Neuroimage. 2019 Jan 1;184:586-598. doi: 10.1016/j.neuroimage.2018.09.061

[14] Visser E, Keuken MC, Forstmann BU, Jenkinson M. Automated segmentation of the substantia nigra, subthalamic nucleus and red nucleus in 7T data at young and old age. Neuroimage. 2016 Oct 1;139:324-336. doi: 10.1016/j.neuroimage.2016.06.039.

[15] Garzón B, Sitnikov R, Bäckman L, Kalpouzos G. Automated segmentation of midbrain structures with high iron content.Neuroimage. 2018 Apr 15;170:199-209. doi: 10.1016 /j.neuroimage.2017.06.016.

[16] Fermin-Delgado R, Roa-Sanchez P, Speckter H, Perez-Then E, Rivera-Mejia D, Foerster B, Stoeter P. Involvement of Globus Pallidus and Midbrain Nuclei in Pantothenate Kinase-Associated Neurodegeneration : Measurement of T2 and T2* Time. Clin Neuroradiol. 2013;23:11-15.

[17] Schneider SA, Dusek P, Hardy J, Westenberger A, Jankovic J, Bhatia KP. Genetics and Pathophysiology of Neurodegeneration with Brain Iron Accumulation (NBIA). Curr Neuropharmacol. 2013 Jan;11(1):59-79. doi: 10.2174/157015913804999469.

[18] Salomão RP, Pedroso JL, Gama MT, Dutra LA, Maciel RH, Godeiro-Junior C, Chien HF, Teive HA, Cardoso F, Barsottini OG. A diagnostic approach for neurodegeneration with brain iron accumulation: clinical features, genetics and brain imaging. Arq Neuropsiquiatr. 2016 Jul;74(7):587-96. doi: 10.1590/0004-282X20 160080.

[19] McNeill A, Birchall D, Hayflick SJ, Gregory A, Schenk JF, Zimmerman EA, Shang H, Miyajima H, Chinnery PF. T2* and FSE MRI distinguishes four subtypes of neurodegeneration with brain iron accumulation. Neurology. 2008 Apr 29;70(18) :1614-9. doi: 10.1212/ 01.wnl. 00003 10985.40 011.d6.

[20] Dusek P, Schneider SA. Neurodegeneration with brain iron accumulation. Curr Opin Neurol. 2012 Aug;25(4):499-506. doi: 10.1097/WCO.0b013e3283550cac.

[21] Zeng J, Xing W, Liao W, Wang X. Magnetic resonance imaging, susceptibility weighted imaging and quantitative susceptibility mapping findings of pantothenate kinase-associated neurodegeneration. J Clin Neurosci. 2019 Jan;59:20-28. doi: 10.1016/ j.jocn. 2018. 10.090.

[22] Manjón JV, Bertó A, Romero JE, Lanuza E, Vivo-Hernando R, Aparici-Robles F, Coupe P. pBrain: A novel pipeline for Parkinson related brain structure segmentation. Neuroimage Clin. 2020;25:102184. doi: 10.1016/ j.nicl. 2020. 10 2184.

[23] Massey LA, Miranda MA, Al-Helli O, Parkes HG, Thornton JS, So PW, White MJ, Mancini L, Strand C, Holton J, Lees AJ, Revesz T, Yousry TA. 9.4 T MR microscopy of the substantia nigra with pathological validation in controls and disease. Neuroimage Clin. 2016 Nov 17;13:154-163. doi: 10.1016/ j.nicl. 2016. 11.015. eCollection 2017.

[24] Zwirner J, Möbius D, Bechmann I, Arendt T, Hoffmann KT, Jäger C, Lobsien D, Möbius R, Planitzer U, Winkler D, Morawski M, Hammer N. Subthalamic nucleus volumes are highly consistent but decrease age-dependently-a combined magnetic resonance imaging and stereology approach in humans. Hum Brain Mapp. 2017 Feb;38(2):909-922. doi: 10.1002/hbm.23427.

[25] Heim B, Krismer F, De Marzi R, Seppi K. J Magnetic resonance imaging for the diagnosis of Parkinson's disease. Neural Transm (Vienna). 2017 Aug;124(8):915-964. doi: 10.1007/s00702-017-1717-8.

[26] Carpenter MB. Connectivity patterns of thalamic nuclei implicated in dyskinesia. Stereotact Funct Neurosurg 1989;52(2-4):79-119. doi: 10.1159/000099491.

[27] Den Dunnen WF. Neuropathological diagnostic considerations in hyperkinetic movement disorders. Front Neurol. 2013 Feb 14;4:7. doi: 10.3389/fneur.2013.00007. eCollection 2013.

[28] Wichmann T. Changing views of the pathophysiology of Parkinsonism. Mov Disord. 2019 Aug;34(8):1130-1143. doi: 10.1002/ mds. 27741

[29] Thomas M, Hayflick SJ, Jankovic Clinical heterogeneity of neurodegeneration with brain iron accumulation (Hallervorden-Spatz syndrome) and pantothenate kinase-associated neurodegeneration. J Mov Disord. 2004 Jan;19(1):36-42. doi: 10.1002/mds.10650.

Citation: *Peter Stoeter et al, Volumes of Midbrain Nuclei in Pantothenate-Kinase Associated Neurodegeneration (PKAN) Dystonia. ARC Journal of Radiology and Medical Imaging. 2020; 4(2): 19-25.*

Copyright: *© 2020 Authors. This is an open-access article distributed under the terms of the Creative Commons Attribution License, which permits unrestricted use, distribution, and reproduction in any medium, provided the original author and source are credited.*